

Photometric Cross-Calibration and Comparison of the SDSS Stripe 82 Standard Stars Catalog with Gaia DR2, Pan-STARRS1, DES and CFIS Catalogs

KARUN THANJAVUR , ¹ ŽELJKO IVEZIĆ , ² SAHAR ALLAM , ³ DOUG TUCKER , ³ AND J. ALLYN SMITH 

¹ Canada

² Department of Astronomy and the DiRAC Institute, University of Washington, 3910 15th Avenue NE, Seattle, WA 98195, USA
³ Batavia

⁴ Dept. of Physics, Engineering & Astronomy, Austin Peay State University, 601 College St., Clarksville, TN 37044, USA

(Received October 5, 2020; Revised Feb 30, 2022; Accepted Feb 31, 2022)

Submitted to AJ

ABSTRACT

We extend the SDSS Stripe 82 Standard Stars Catalog reported in Ivezić et al. (2007) with post-2007 SDSS imaging data. Their catalog lists averaged SDSS *ugriz* photometry for about a million stars brighter than $r \sim 22$. The new version released here is based on 2-3 times more measurements per star, resulting in 1.4-1.7 times smaller random errors than in the original catalog, and about three times as small as for individual SDSS runs. Random errors in the new catalog are below 0.01 mag for stars brighter than 20.0, 21.0, 21.0, 20.5, and 19.0 in *ugriz*, respectively. We use Gaia DR2 Gmag photometry to derive gray photometric zeropoint corrections, as functions of R.A. and Declination, for the SDSS catalog, and Gaia's BP-RP colors to derive corrections in the *ugiz* bands, relative to the *r* band. We test the quality of recalibrated SDSS photometry by comparing it to Gaia DR2, Pan-STARRS1, DES and CFIS photometry for the same stars. This multi-survey comparison indicates that the spatial variation of photometric zero points in the updated SDSS catalog is well below 0.01 mag (rms), with typical values of 3-7 millimag in the R.A. direction and 1-2 millimag in the Declination direction, except for the *u* band with a scatter of about 6 millimag. We also report a few minor photometric problems with all the surveys considered here, including Gaia DR2. Due to its large size and cross-checks with other surveys, this SDSS catalog can be used to robustly calibrate or test *ugriz* photometry below 1% level, for example, as part of the commissioning phase of the Rubin Observatory Legacy Survey of Space and Time.

Keywords: catalogs – instrumentation: photometers – methods: data analysis – standards – surveys – techniques: photometric

1. INTRODUCTION

Modern multi-band photometric sky surveys aim to deliver measurements accurate¹ at the 1% (0.01 mag) level, to enable cosmological and other high-precision measurements (e.g., the Vera Rubin Observatory Legacy Survey of Space and Time, Ivezić et al. 2019). Photometric data are usually calibrated using sets of standard stars whose brightness is known from previous work. One of the largest catalogs with sub-percent measurement precision and optical multi-band *ugriz* photometry was constructed by averaging multi-epoch data for about a million stars collected by the Sloan Digital Sky Survey (SDSS, York et al. 2000) in a 300 deg² region known as SDSS Stripe 82 (Ivezić et al. 2007, hereafter I007). The SDSS *ugriz* photometric system is now in use at many observatories worldwide and this catalog² (hereafter I007 catalog) has been used both for calibration and testing of other surveys.

Corresponding author: Karun Thanjavur
karun@uvic.ca

¹ Except for zeropoint offsets from the AB magnitude scale, discussed in Section XXX.

² Available from <http://faculty.washington.edu/ivezic/sdss/catalogs/stripe82.html>

After the completion of I007 catalog, SDSS has obtained additional imaging data, about 2-3 times more measurements per star depending on its sky position within Stripe 82. This increased number of data points can result in averaged photometry with 1.4-1.7 times smaller random errors (precision) than in the original catalog (and about three times as small as for individual SDSS runs). In addition, the availability of photometric data from recent wide-field surveys such as the Dark Energy Survey (Dark Energy Survey Collaboration et al. 2016), Pan-STARRS (Kaiser et al. 2010) and Gaia (Gaia Collaboration et al. 2018), enables a much more detailed and robust cross-calibration, including correcting for residual photometric zeropoint errors in SDSS flat-fielding (e.g., a saw-tooth pattern, as a function of Declination, was reported by Betoule et al. 2013; see their Fig. 23). These are the main reasons that motivated us to construct an updated version of the SDSS Standard Star Catalog.

We describe datasets used in our analysis in §2, and the construction of the new catalog and its analysis in §3. Our results are summarized and discussed in §4.

2. DATASETS

2.1. SDSS Stripe 82 Imaging Data

In the SDSS survey, Stripe 82 is a contiguous, 300 deg^2 equatorial region, which stretches between $-60^\circ \leq RA \leq 60^\circ$ [20h to 4h], and $-1.266^\circ \leq Dec \leq 1.266^\circ$. Following the initial concerted effort by the SDSS collaboration between 2001 and 2008 to map this region repeatedly to a forecast imaging depth, $r \leq 22$, several other surveys in various wavebands too have targeted this same patch of sky to provide a rich multi-wavelength dataset suitable for a variety of investigations. SDSS observations too have continued in this region (e.g., the SDSS-II search for supernovae, Frieman et al. 2008), resulting in an imaging depth deeper than what was initially planned.

Data from the SDSS imaging camera (Gunn et al. 1998) are collected in drift-scan mode. The images that correspond to the same sky location in each of the five photometric bandpasses (these five images are collected over ~ 5 minutes, with an exposure time of 54 seconds for each band) are grouped together for simultaneous processing as a field. A field is defined as a 36 seconds (1361 pixels) stretch of drift-scanning data from a single column of CCDs (sometimes called a scan line; for more details, see I007 and references therein).

2.1.1. The 2007 SDSS Standard Star Catalog

The SDSS standard star catalog published by I007 (version 2.6) was constructed by averaging multiple SDSS photometric observations (at least four per band, with a median of 10) in the *ugriz* system. The catalog includes 1.01 million non-variable unresolved objects. The measurements for individual sources have random photometric errors below 0.01 mag for stars brighter than 19.5, 20.5, 20.5, 20, and 18.5 in *ugriz*, respectively (about twice as good as for individual SDSS runs). Several independent tests of the internal consistency suggested that the spatial variation of photometric zero points is not larger than ~ 0.01 mag (rms).

2.1.2. Post-2007 SDSS data

In this work, we have used the SDSS Data Release 15 (DR15) as available in April 2019 (Blanton et al. 2017). In DR15, the Stripe 82 region is covered by 118 *runs*, which include 32,292 fields, each with observations in the five *ugriz* SDSS filters. Using our programmatic query tool, we obtained the processed data for all these runs from the DR15 public database. In the database, the data are presented as individual FITS tables, named `photoObj_<run>_<camcol>_<field>.fits`. From each table, we extracted photometric and astrometric quantities, time of observation, and several ancillary data for all the objects into a formatted, 107-column wide ascii master file for further processing.

The objects in each of these data files were then matched with the standard stars in the I007 catalog using their mean sky positions (R.A. and Declination) and a matching radius of 0.5 arcsec. For matching, only deblended objects (`nchild=0`), lying between rows $64 < objc_rowc < 1424$ in each field, were selected to avoid poor photometry due to blending or lying close to edges of the CCD. From these matched objects, only those with photometric error < 0.1 mag were selected to compute photometric zeropoint offsets between the I007 catalog and DR15. These offsets were obtained independently for all runs and fields, and in all five filters, and applied to bring our DR15 based catalog to the same photometric scale as the I007 catalog – in essence, we have re-calibrated photometry for all Stripe 82 runs in DR15 using the I007 catalog. In addition, the MJD and fractional MJD of observation were computed using the median of the TAI values (the GPS based time reported by the SDSS Apache Point Observatory) for these matched objects. In the final step, the photometric, astrometric and other details for each of these matched standard stars

were written to independent (one per star) light curve files. Further processing of these light curves is described in Section 3.1.

All these processing steps were completed on a single quad-core desktop needing several days of processing. The final dataset, consisting of all the light curves in the five *ugriz* filters for the 1,006,849 standard stars in the I007 catalog resulted in \sim 20 GB of tabular data. To make file search and access fast, the data have been chunked into sub-directories, each spanning 1 deg in RA, and 0.1 deg in Dec (a "poor-man's" two-dimensional tree structure). These light curve data files can be made available as a single tarball by emailing the contact author.

2.2. *Gaia Data Release 2 (DR2) Data*

The second Gaia Data Release, Gaia DR2, includes astrometry, photometry, radial velocities, and information on astrophysical parameters and variability, for sources brighter than magnitude Gmag \sim 21 (Gaia Collaboration et al. 2018). This dataset is based on the first 22 months of the mission and includes celestial positions and the apparent brightness in the broad-band G (Gmag hereafter) for approximately 1.7 billion sources. This data release also contains two additional broad-band magnitudes, the BP (330-680 nm) and RP (630-1050 nm), for 1.4 billion sources.

Gaia DR2 photometry is superior to ground-based photometry for sources with sufficient signal-to-noise ratio, and we use it to derive zeropoint corrections for SDSS photometry, as described in Section 3.

2.3. *Pan-STARRS (PS1) Data*

KT to fill in details

Pan-STARRS (Kaiser et al. 2010)

2.4. *Deep Energy Survey (DES) Data*

DT/SA to fill in details

Dark Energy Survey (Dark Energy Survey Collaboration et al. 2016)

Old text from Doug, needs editing:

We use the Dark Energy Survey Data Release 1 (DES DR1; Abbott et al. 2018) public data set. DES DR1 object catalog consists \sim 400 million objects covering 5000deg^2 of the southern Galactic cap in the five DES grizY filters. The 10σ Depth in grizY is 24.33, 24.08, 23.44, 22.69, and 21.44 mag, and median point-spread function is 1.12, 0.96, 0.88, 0.84, and 0.90 FWHM in grizY respectively, a photometric precision of $<1\%$ in all bands. The astrometric precision of 151 mas (for a full discussion about the astrometric solution and the accuracy see Abbott et al. 2018). We made use of the DES DR1 access through the NOAO Data Lab (<http://datalab.noao.edu>) via Table Access Protocol (TAP) service, and downloaded the overlapping area with S82. We selected stars via SPREAD_MODEL and SPREADERR_MODEL (in the i-bands; in particular EXTENDED_COADD ≤ 1 as described in eq. 2 of Abbott et al. 2018), with WAVG_MAG_PSF in AB mag keeping all good data with IMAGFLAGS_ISO==0 (in the i-bands).

2.5. *Canada-France Imaging Survey (CFIS) Data*

Emails from SGwyn to fill in details

2.6. OLD TEXT FROM DOUG: Comparison of SSC 2020 vs DES DR1

We use the Dark Energy Survey Data Release 1 (DES DR1; Abbott et al. 2018) public data set. DES DR1 object catalog consists ~ 400 million objects covering 5000deg^2 of the southern Galactic cap in the five DES grizY filters. The 10σ Depth in grizY is 24.33, 24.08, 23.44, 22.69, and 21.44 mag, and median point-spread function is 1.12, 0.96, 0.88, 0.84, and 0.90 FWHM in grizY respectively, a photometric precision of $<1\%$ in all bands. The astrometric precision of 151 mas (for a full discussion about the astrometric solution and the accuracy see Abbott et al. 2018). We made use of the DES DR1 access through the NOAO Data Lab (<http://datalab.noao.edu>) via Table Access Protocol (TAP) service, and downloaded the overlapping area with S82. We selected stars via SPREAD_MODEL and SPREADERR_MODEL (in the i-bands; in particular EXTENDED_COADD ≤ 1 as described in eq. 2 of Abbott et al. 2018), with WAVG_MAG_PSF in AB mag keeping all good data with IMAFLAGS_ISO==0 (in the i-bands).

After matching both catalogs were final data set contains 619,741 stars, with mean separation $0.135'' \pm 0.094''$, with a median of $0.116''$. We transform the DES to the SDSS system following Drlica-Wagner 2017, cf. APPENDIX A.4 eq. A9–A12). In particularly we used:xdse

$$g_{sdss} = g_{des} - 0.1174 \times (g - r)_{des} + 0.0217 \quad (1)$$

$$r_{sdss} = r_{des} - 0.0115 \times (g - r)_{des} + 0.0201 \quad (2)$$

$$i_{sdss} = i_{des} - 0.3891 \times (i - z)_{des} + 0.0067 \quad (3)$$

$$z_{sdss} = z_{des} + 0.1307 \times (i - z)_{des} + 0.0114. \quad (4)$$

SSA Added a new Dir for some comparison Figs DT/SA to fill in details

2.7. Comparison of SSC 2020 vs PSI

KT to fill in details

2.8. Comparison of SSC 2020 vs CFIS

ZI/SG to fill in details

2.9. Comparison of SSC 2020 vs HSC

KT to fill in details

2.10. Comparison of SSC 2020 vs Galex

SA to fill in details

3. THE CONSTRUCTION AND ANALYSIS OF THE NEW V3.4 CATALOG

We first describe the construction of the new SDSS catalog and derivation of photometric zeropoint corrections using Gaia DR2 data, and then compare the resulting photometry to Gaia DR2, DES, Pan-STARRS and CFIS catalogs.

3.1. *The construction of raw SDSS catalog from light curves*

Given light curve data files described in Section 2.1.2, we computed the median and mean magnitudes, their formal uncertainties and χ^2 (assuming constant brightness) for all stars, in all five bands. Due to more observational epochs in DR15, the new data are more sensitive to variability; following I007, we applied $\chi^2 > 3$ in the *gri* bands, as well as requirements for at least 4 epochs in the same three bands and the formal uncertainty of the mean *r* band magnitude below 0.05 mag. These selection criteria recovered 98.5% stars from the original catalog, resulting in a new catalog with 991,472 stars.

Figure 1 compares the numbers of epochs for matched stars and their formal uncertainties of the mean *r* band magnitude. The new 2020 catalog has about 2-3 times more measurements per star, depending on its sky position within Stripe 82. Consequently, formal photometric uncertainties (“random errors”) are about 1.4-1.7 times smaller. This raw catalog is labeled version v3.1, and is publicly available from the same website³ as the original 2007 catalog.

A star-by-star comparison of the photometry between the old and new catalogs is discussed in Section 3.3.

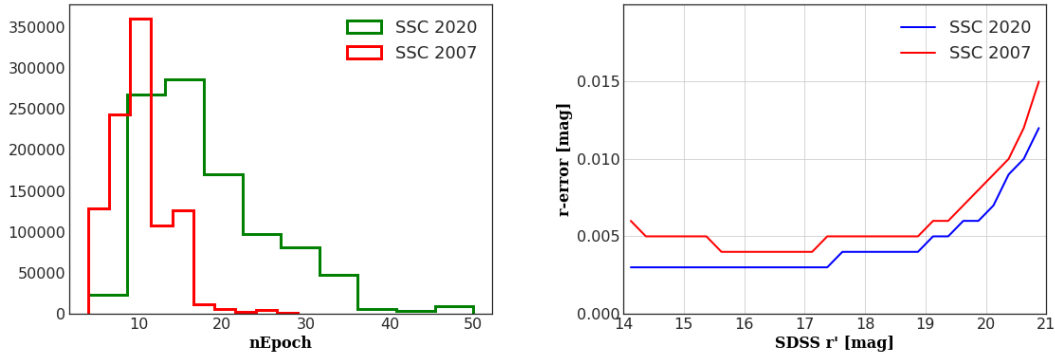


Figure 1. *Left:* A comparison of the number of observational epochs for matched stars in the 2020 versus 2007 Standard Star Catalog (SSC). *Right:* A comparison of the median formal *r* band photometric uncertainties of matched objects in the 2020 versus 2007 SSC, as a function of their mean *r* magnitudes.

3.2. *The derivation of photometric zeropoint corrections using Gaia DR2 data*

The variation of photometric zeropoints with position on the sky in the I007 catalog (see their eq. 4) was constrained using a combination of stellar colors (the principal axes in color-color diagrams, for details see Ivezić et al. 2004) and a standard star network (Smith et al. 2002). It is likely that residual errors in zeropoint calibration (e.g., a saw-tooth pattern, as a function of Declination, was reported by Betoule et al. 2013; see their Fig. 23) can be further minimized using uniformly calibrated space-based photometry from Gaia Data Release 2 (DR2).

3.2.1. *Positional matching of the SDSS and Gaia catalogs*

Naively, one would positionally match the SDSS and Gaia DR2 catalogs using a matching radius of about 0.3 arcsec because SDSS positions are accurate to better than 0.1 arcsec per coordinate (rms) for sources with $r < 20.5$ mag (Pier et al. 2003). However, observational epochs are sufficiently different that stellar proper motions need to be accounted for; indeed, we find a very strong correlation between the SDSS-Gaia positional differences and proper motions published in the Gaia DR2 catalog (see the left panel in Figure 2). After accounting for proper motions, the positions agree at the level of ~ 28 milliarcsec (robust⁴ rms, per coordinate). The residual differences are dominated

³ <http://faculty.washington.edu/ivezic/sdss/catalogs/stripe82.html>

⁴ We use robust estimator of standard deviation computed as $\sigma_G = 0.741 * (q_{75} - q_{25})$, where q_{25} and q_{75} are the 25% and 75% quantiles, and the normalization factor 0.741 assures that σ_G is equal to standard deviation for normal (Gaussian) distribution.

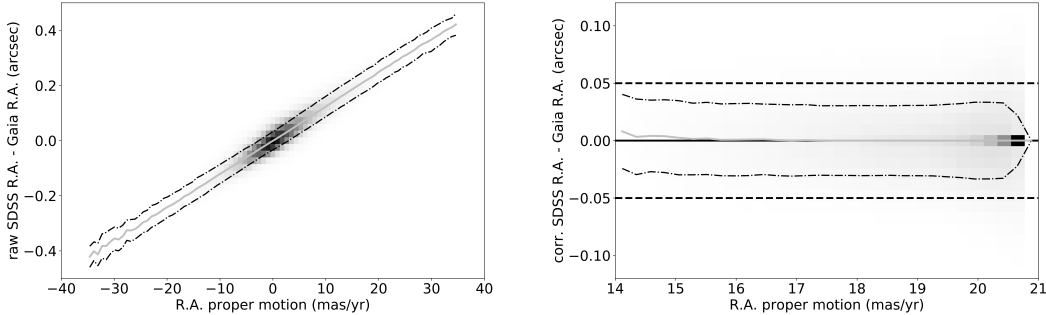


Figure 2. The left panel shows the R.A. difference between SDSS and Gaia vs. R.A. proper motion reported by Gaia DR2. The solid line shows the median difference in bins of proper motion and the dashed lines mark the $\pm\sigma_G$ envelope around the medians, where σ_G is the robust standard deviation. The right panel shows the R.A. difference after correcting using the best-fit R.A. difference vs. proper motion curve, as a function of the SDSS r magnitude. As evident, the residual differences are dominated by systematic errors in SDSS astrometry at the level of ~ 28 milliarcsec (note that there is no increase with magnitude). Analogous plots for Declination quantities are similar.

by systematic errors in SDSS astrometry because there is no increase of this rms with magnitude (see the right panel in Figure 2), and because the contribution of Gaia’s astrometric measurement uncertainties is negligible. The implied SDSS astrometric accuracy of ~ 28 milliarcsec is substantially better than “ < 0.1 arcsec reported by Pier et al. (2003), but note that here we used positions “averaged” over typically ~ 20 SDSS runs (see the left panel in Figure 1).

3.2.2. *Gaia-based photometric zeropoint corrections*

Gaia DR2 reported Gmag magnitudes, which approximately span the SDSS *griz* bandpasses, and BP and RP magnitudes, which approximately correspond to the blue and red halves of the Gmag bandpass. We first used Gmag data to derive “gray” zeropoint corrections (applied to all five SDSS bands), and then use the BP-RP color to derive zeropoint corrections for the *ugiz* bands, relative to the r band.

The basic idea is simple: use Gaia’s Gmag, $\text{Gmag}_{\text{GaiaDR2}}$, and the SDSS *gri* magnitudes to derive synthetic Gmag magnitudes based on SDSS data, $\text{Gmag}_{\text{SDSS}}$; bin the $\Delta\text{Gmag} = (\text{Gmag}_{\text{SDSS}} - \text{Gmag}_{\text{GaiaDR2}})$ residuals by R.A. and Dec, and use the median residuals per bin as the gray correction for SDSS photometry (as functions of R.A. and Dec). Similarly, use Gaia’s BP-RP color to derive synthetic $u-r$, $g-r$, $r-i$ and $r-z$ colors, and used the median residuals per bin as zeropoint corrections for the *ugiz* bands.

Given a large number of matched stars ($\sim 400,000$), and a large number of color combinations, we do not attempt to derive analytic fits for synthetic magnitudes and colors but instead use 0.05 mag narrow color bins and linear interpolation between the bins. We have verified that even sixth-order polynomial fits do not provide better results than this simple numerical approach. An example of such a transformation is shown in Figure 3.

The variation of Gmag residuals shows two interesting features. First, there is a sharp “jump” by about 3 millimag at $\text{Gmag} \sim 16$. This jump was a known (and larger problem) in Gaia Data Release 1, but appears not entirely fixed in DR2. The second “feature” is a large ($\sim 0.01 - 0.02$ mag) discrepancy at the faint end: about ~ 10 millimag at $\text{Gmag} = 19.5$ and ~ 20 millimag at $\text{Gmag} = 20.5$. A comparison of the SDSS catalog with Pan-STARRS and DES catalogs (see Section 3.5 and Figure 15) strongly suggests that the origin of this discrepancy is a bias in Gaia’s Gmag photometry at the faint end, rather than a problem with SDSS catalog (offsets between the SDSS and DES photometry are $< 1 - 2$ millimag at $\text{Gmag} \sim 20.5$).

Given these two features, we limit the calibration sample to the $16 < \text{Gmag} < 19.5$ magnitude range. We further restrict calibration stars to the $0.4 < g-i < 3.0$ color range (approximately A0 to M5 spectral range), yielding a sample of $\sim 372,000$ stars. The behavior of median Gmag residuals per R.A. and Declination bin is shown in Figures 5 and 6.

Except for a few degrees long region at the edge of Stripe 82 (R.A. > 55 deg), the SDSS photometric zeropoints are remarkably stable with respect to R.A.; the scatter is only 3.5 millimag. On the other hand, there are clear deviations in Declination direction, which clearly map to the 12 scanning strips that fill Stripe 82. We note that discrepancies never exceed 0.01 mag (with a scatter of 6.2 millimag), which was the claimed accuracy of the I007 catalog. Thanks

to a large number of stars in the sample, and well calibrated Gaia’s photometric zeropoints across the sky, we can now constrain SDSS zeropoints with a precision of about 1 millimag per 0.01 degree wide Declination bin.

The residuals shown in Figures 5 and 6 are applied as “gray” zeropoint corrections to $ugriz$ magnitudes, as functions of R.A. and Declination, to all 991,472 stars in the catalog. This catalog version was labeled v3.1, and it is publicly available⁵.

In the next re-calibration step, we derive synthetic $u - r$, $g - r$, $r - i$ and $r - z$ colors from Gaia’s BP-RP color, using the same binning procedure as we used above for Gmag– r vs. $g - i$ variation (see Figure 3). An example of color residuals is shown in Figure 7. The median residuals per R.A. and Declination bins are then used as zeropoint corrections for the $ugiz$ bands. The robust standard deviation for all zeropoint corrections is listed in Table 1.

The largest corrections were derived for the u band. Given that Gaia’s BP-RP color does not strongly constrain the u band flux, we used the CFIS catalog (see Section 2.5) as an independent verification test. We verified that zeropoint errors in the SDSS catalog implied by Gaia’s and CFIS data agree in Declination direction, but found inconsistencies for R.A. bins. For this reason, we only applied u band correction in Declination direction. The plausible u band zeropoint errors in the new catalog are further discussed in Section 3.6. This final catalog version was labeled v3.4, and it is also publicly available.

Table 1. The robust standard deviation for binned SDSS-based vs. Gaia-based color residuals^a.

Color	rms for R.A.	rms for Dec
gray (Gmag)	3.5	6.2
$u - r$	0.0 ^b	20.4
$g - r$	4.0	4.2
$r - i$	4.1	3.2
$r - z$	7.4	2.9

^aThe robust standard deviation is estimated using interquartile range. The units are millimag.

^bFor the u band, we could not confirm the R.A. behavior of Gaia-based zeropoint correction with the CFIS data and didn’t apply it. The large u band correction as a function of Declination was validated with the CFIS data (see Section 3.6).

3.3. Comparison of the SDSS v2.6 and v3.4 catalogs

The v2.6 (“old”) SDSS Standard Star Catalog has been extensively used (e.g., Frieman et al. 2008), and here we briefly analyze differences between the v3.4 (“new”) and v2.6 magnitudes to inform the future users about catalog consistency. In our analysis, we first compare v2.6 and v3.4 magnitudes of individual stars and bin the differences by R.A., Declination and magnitude.

On average, both catalog versions are on the same magnitude scale (the median $ugriz$ magnitude differences for all stars are zero by construction). There are no systematic offsets when binned by magnitude, as illustrated in Figure 9. The most obvious differences appear when magnitude differences are binned by Declination. An example is shown in Figure 9, where the periodicity of residuals corresponds to the field-of-view size for the SDSS Photometric Calibration Telescope (Smith et al. 2002). The standard deviation for median values per bin is 6.8 millimag, with extreme values about 0.01 mag. It is likely that systematic errors in the calibration star network photometry were propagated through

⁵ See <http://faculty.washington.edu/ivezic/sdss/catalogs/stripe82.html>

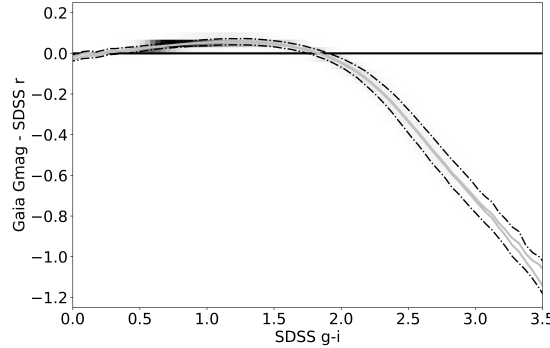


Figure 3. The variation of the difference between Gaia’s Gmag magnitude from Data Release 2 and SDSS r magnitude with the SDSS $g - i$ color. The color map illustrates the distribution of $\sim 393,000$ matched stars with $16 < \text{Gmag} < 19.5$. The two (barely distinguishable) solid lines represent the median values \pm uncertainty of the median for 0.05 mag wide $g - i$ bins. The short-dashed lines show the median values \pm the robust standard deviation for each bin. The horizontal solid line at zero is added to guide the eye. The mean of the two solid lines is used to derive the gray zeropoint correction, as a function of R.A. and Declination.

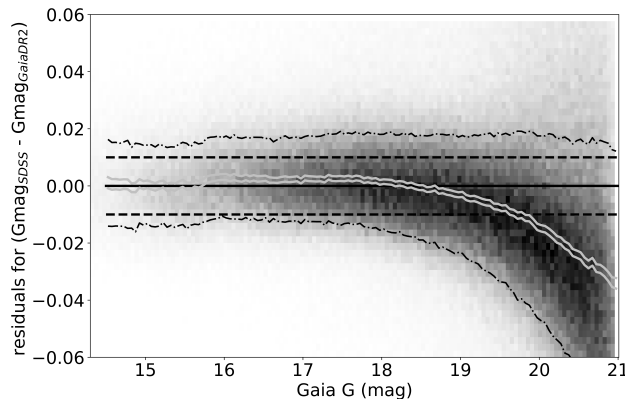


Figure 4. The variation of the residuals between Gaia’s Gmag from Data Release 2 and synthetic Gmag values generated using SDSS gri photometry. The two solid lines represent the median values \pm uncertainty of the median for each 0.05 mag wide Gmag bin. The short-dashed lines show the median values \pm the robust standard deviation for each bin. The horizontal solid and long-dashed lines at zero and ± 0.01 mag, respectively, are added to guide the eye. Note the jump by about 3 millimag at $\text{Gmag} \sim 16$ – this jump was a known and larger problem in Gaia Data Release 1, and apparently not entirely fixed in DR2. Note also large ($\sim 0.01 - 0.02$ mag) discrepancy at the faint end – a comparison of the SDSS catalog with Pan-STARRS and DES catalogs (see Figure 15) suggests that its origin is a bias in Gaia’s photometry at the faint end, rather than a problem with SDSS photometry.

“flat-field corrections” discussed by I007 to the v2.6 catalog. We note that these errors, now found thanks to Gaia catalogs, are well within the claimed photometric accuracy by both I007 and Smith et al. (2002).

Given the quality of Gaia photometry, there should be no doubt that SDSS $ugriz$ photometry reported in the new v.3.4 catalog is superior to the old v2.6 catalog. Nevertheless, we perform additional tests, based on the position of the stellar locus in the $g - r$ vs. $u - g$, $r - i$ vs. $g - r$ and $i - z$ vs. $r - i$ color-color diagrams (Ivezić et al. 2004). The tests are based on the second principal color for the blue part of the stellar locus, whose median should not deviate from zero by construction. Figure 10 compares the behavior of the w color for the old v2.6 and new v3.4 catalog and demonstrates that the gri photometry is better calibrated in the latter. The behavior of the s and y colors for the new catalog is shown in Figure 11. Based on these tests, we find that the contribution of the zeropoint errors is < 5 millimag to gri photometry, and < 10 millimag for the u and z bands.

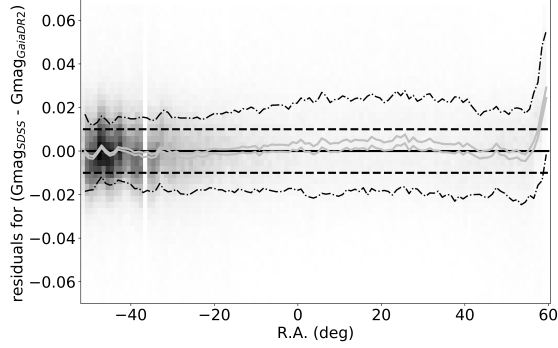


Figure 5. The R.A. variation of the residuals between Gaia’s Gmag from DR2 and synthetic Gmag values generated using SDSS *gri* photometry. The color map illustrates the distribution of $\sim 372,000$ matched stars with $16 < \text{Gmag} < 19.5$ and $0.4 < g - i < 3.0$. The two solid lines represent the median values \pm uncertainty of the median for 1 degree wide R.A. bins. The short-dashed lines show the median values \pm the robust standard deviation for each bin. The horizontal solid and long-dashed lines at zero and ± 0.01 mag, respectively, are added to guide the eye. The mean of the two solid lines is the gray correction, as a function of R.A., applied to the SDSS *ugriz* magnitudes. The standard deviation for the applied correction is 3.5 millimag.

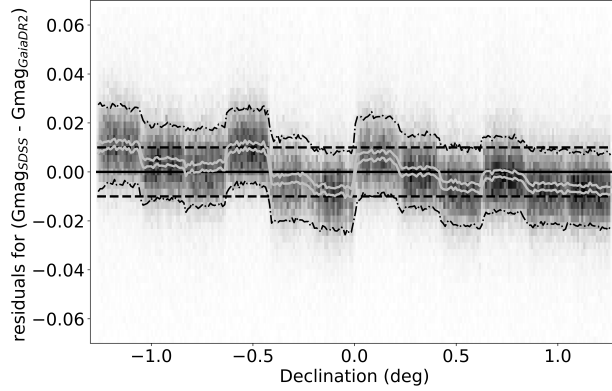


Figure 6. Analogous to Figure 5, except that here results are shown for 0.01 degree wide Declination bins. The 12 clearly visible regions correspond to two SDSS scans (in R.A. direction) and six CCD columns in the SDSS camera. The standard deviation for the applied correction is 6.2 millimag, with a maximum absolute value of ~ 0.01 mag.

3.4. Comparison of the new v3.4 SDSS catalog and Gaia DR2 catalog

3.5. Comparison of the new v3.4 SDSS catalog with DES and Pan-STARRS catalogs

Conclusion: in RA: 3-7 millimag, Dec: 1-2 millimag (CFIS: 6 millimag in u)

3.6. Comparison of the new v3.4 SDSS catalog and u band data from the CFIS catalog

CFIS: as a function of RA, the maximum u band zeropoint offset is limited to < 0.02 mag, with rms of 17 millimag.

4. DISCUSSION AND CONCLUSIONS

ACKNOWLEDGMENTS

Funding for the SDSS and SDSS-II has been provided by the Alfred P. Sloan Foundation, the Participating Institutions, the National Science Foundation, the US Department of Energy, the National Aeronautics and Space Administration, the Japanese Monbukagakusho, the Max Planck Society, and the Higher Education Funding Council for England. The SDSS Web site is <http://www.sdss.org>.

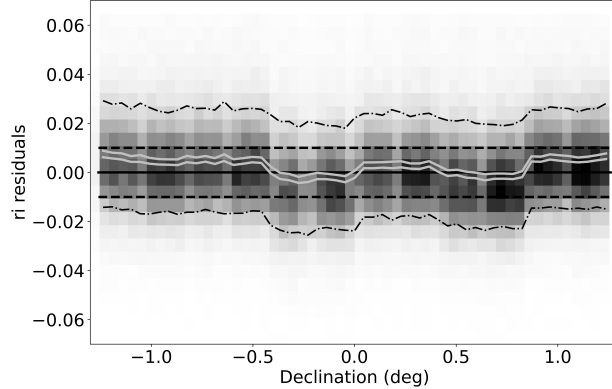


Figure 7. Analogous to Figure 6, except that here residuals correspond to differences between the SDSS $r - i$ color and a synthetic $r - i$ color generated using Gaia’s $BP - RP$ color. Note the signature of SDSS camera columns at the level of a few millimags. The standard deviation for the binned medians is 3.2 millimag (for other bands, please see Table 1).

Table 2. The robust standard deviation for magnitude differences between the v2.6 (old) and v3.4 (new) catalogs.

Band	rms for R.A.	rms for Dec
u	2.3 ^a	25.5
g	4.5	9.4
r	2.0	7.0
i	5.3	6.5
z	8.9	8.4

^aFor the u band, the scatter in R.A. direction is due to more observations in v3.4 than in v2.6, rather than zeropoint correction.

Table 3. The robust standard deviation for binned median magnitude differences between the new v3.4 SDSS catalog, and DES and Pan-STARRS1 (PS1) catalogs (millimag).

Band	DES R.A.	DES Dec	PS1 R.A.	PS1 Dec
g	5.1	1.8	3.4	1.4
r	4.1	0.8	2.6	0.7
i	7.3	1.6	3.2	1.0
z	13.6	3.6	6.8	2.3

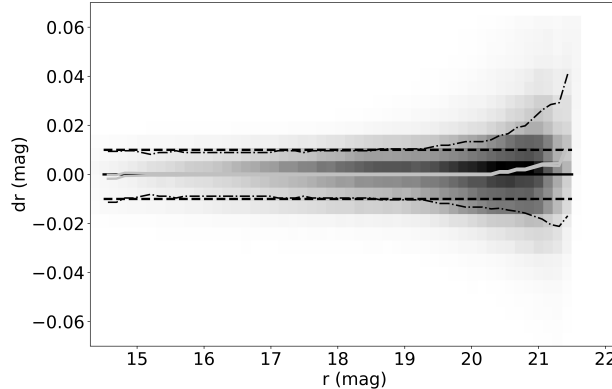


Figure 8. Analogous to Figure 9, except that here the r band differences are shown as a function of the r band magnitude. The scatter of median values per bin is 1.9 millimag. The scatter of individual values is ~ 0.01 mag for $r < 20$, and it is due to more data in the new catalog.

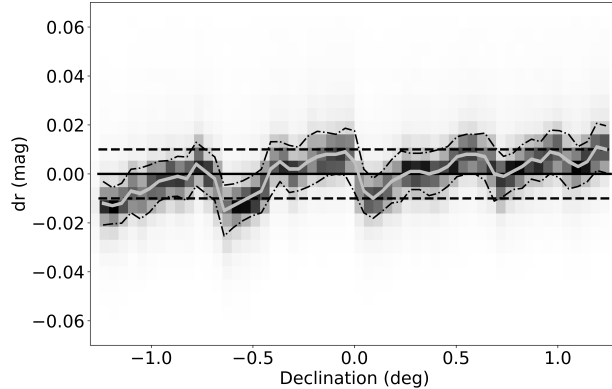


Figure 9. The differences between r band magnitudes listed in the v2.6 and v3.4 SDSS Standard Star catalogs. The size of the four regions corresponds to the field-of-view size of the SDSS Photometric Calibration Telescope. The standard deviation for median values per bin is 6.8 millimag, with extreme values about 0.01 mag. The scatter of binned medians in R.A. direction is much smaller – 2.0 millimag. For statistics in other bands, please see Table 2.

Software: numpy (Oliphant 2006), matplotlib (Hunter 2007), scipy (Jones et al. 2001–), astropy (Astropy Collaboration et al. 2013, 2018), astroML (VanderPlas et al. 2012).

REFERENCES

- Astropy Collaboration, Robitaille, T. P., Tollerud, E. J., et al. 2013, A&A, 558, A33, doi: [10.1051/0004-6361/201322068](https://doi.org/10.1051/0004-6361/201322068)
- Astropy Collaboration, Price-Whelan, A. M., Sipőcz, B. M., et al. 2018, AJ, 156, 123, doi: [10.3847/1538-3881/aabc4f](https://doi.org/10.3847/1538-3881/aabc4f)
- Betoule, M., Marriner, J., Regnault, N., et al. 2013, A&A, 552, A124, doi: [10.1051/0004-6361/201220610](https://doi.org/10.1051/0004-6361/201220610)
- Blanton, M. R., Bershadsky, M. A., Abolfathi, B., et al. 2017, AJ, 154, 28, doi: [10.3847/1538-3881/aa7567](https://doi.org/10.3847/1538-3881/aa7567)
- Dark Energy Survey Collaboration, Abbott, T., Abdalla, F. B., et al. 2016, MNRAS, 460, 1270, doi: [10.1093/mnras/stw641](https://doi.org/10.1093/mnras/stw641)
- Frieman, J. A., Bassett, B., Becker, A., et al. 2008, AJ, 135, 338, doi: [10.1088/0004-6256/135/1/338](https://doi.org/10.1088/0004-6256/135/1/338)
- Gaia Collaboration, Brown, A. G. A., Vallenari, A., et al. 2018, A&A, 616, A1, doi: [10.1051/0004-6361/201833051](https://doi.org/10.1051/0004-6361/201833051)
- Gunn, J. E., Carr, M., Rockosi, C., et al. 1998, AJ, 116, 3040, doi: [10.1086/300645](https://doi.org/10.1086/300645)

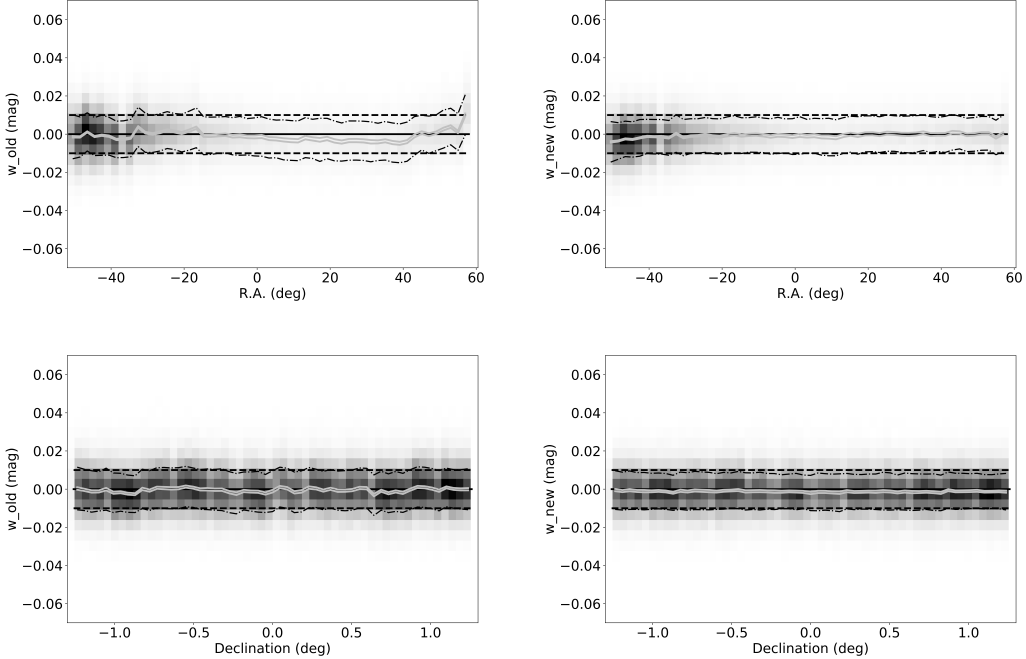


Figure 10. A comparison of the w color, the second principal color in the SDSS $r - i$ vs. $g - r$ color-color diagram, behavior for the v2.6 (left) and v3.4 (right) catalogs. The standard deviation of the median w values binned by R.A. and Dec is 2.6 millimag and 1.1 millimag for v2.6 and 1.0 millimag and 0.3 millimag for v3.4, respectively.

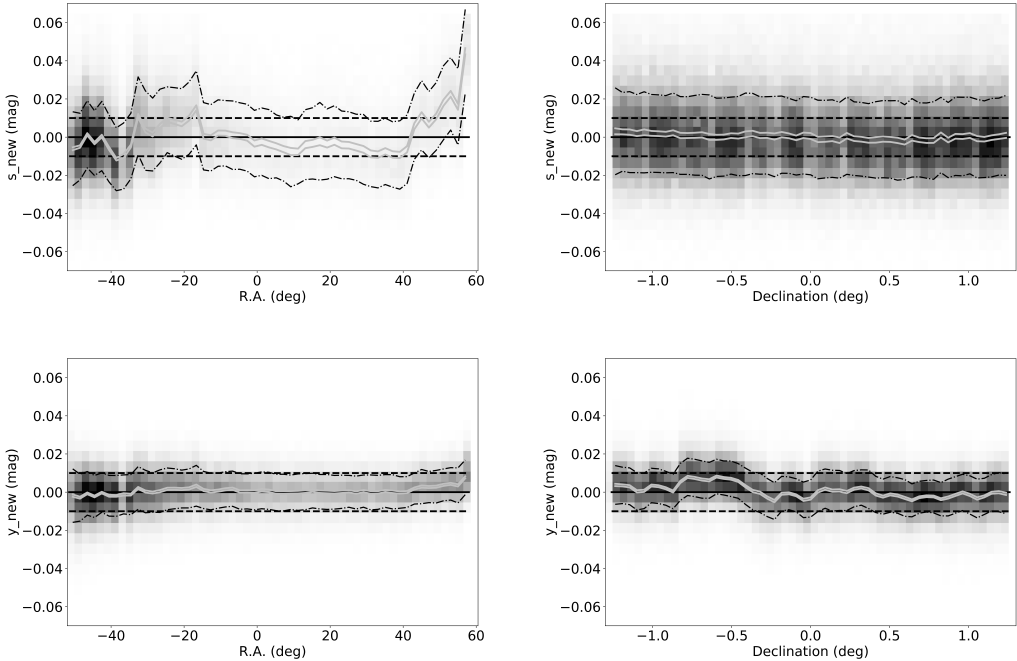


Figure 11. The behavior of the s color (top two panels), the second principal color in the SDSS $g - r$ vs. $u - g$ color-color diagram, and the y color (bottom two panels), the second principal color in the SDSS $i - z$ vs. $r - i$ color-color diagram, for the new v3.4 catalog. The standard deviation of the median s values binned by R.A. and Declination is 9.8 millimag and 1.3 millimag, respectively, and 1.8 millimag and 3.4 millimag for the y color.

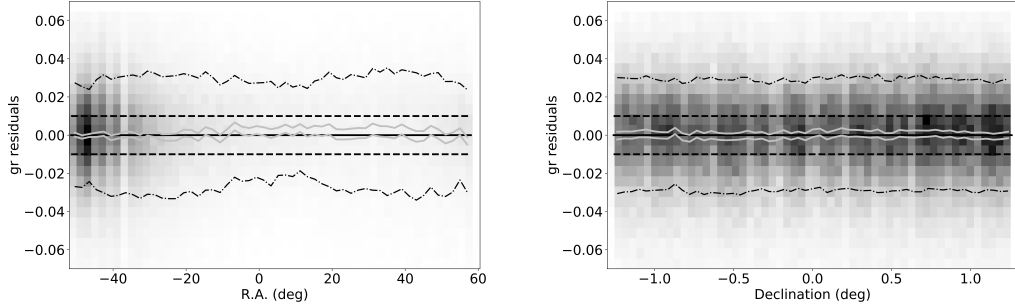


Figure 12. Left: analogous to Figure 5, except that here residuals between the SDSS $g - r$ color from the v3.4 catalog and a synthetic $g - r$ color generated using Gaia's $BP - RP$ color are shown. The binned median scatter is 1.6 millimag. Right: the $g - r$ residuals are shown as a function of Declination. The binned median scatter is 0.8 millimag.

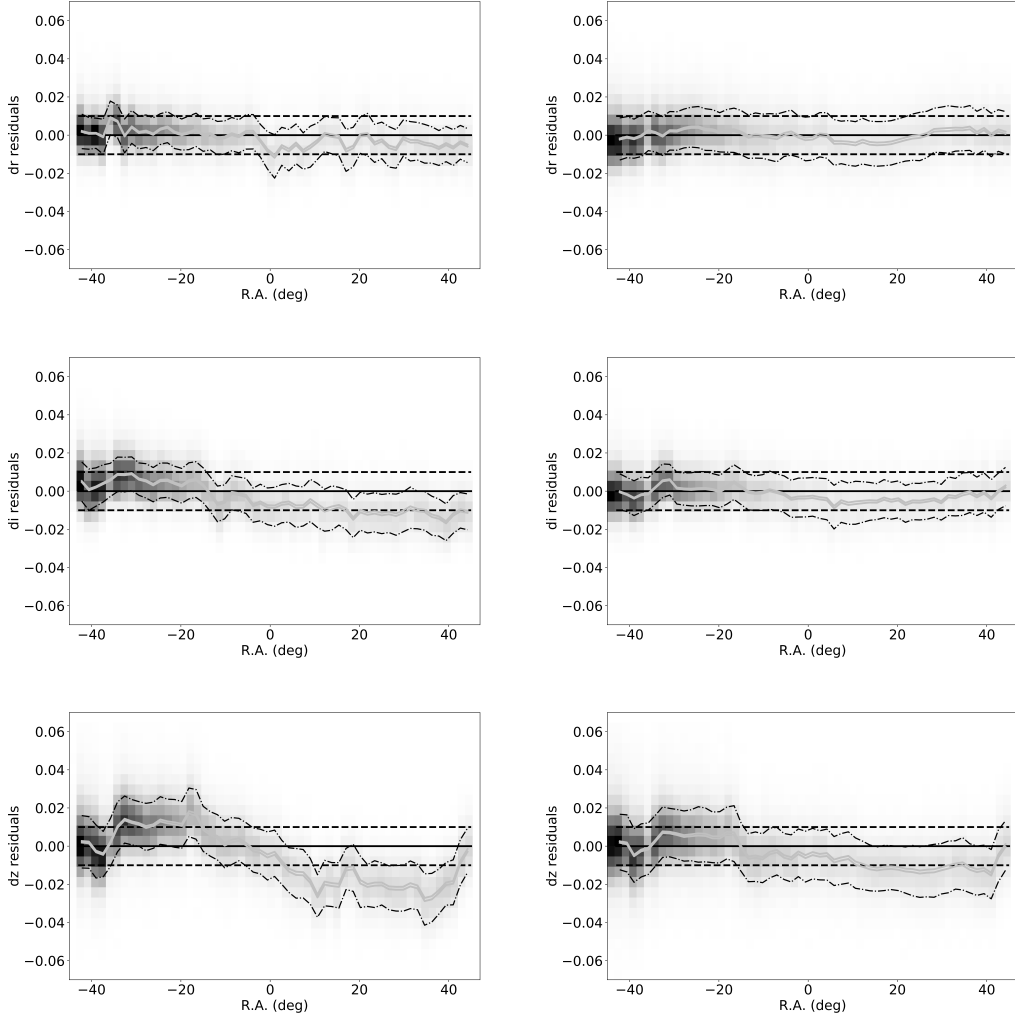


Figure 13. A comparison of the magnitude differences between the SDSS v3.4 catalog and DES (left) and Pan-STARRS (right) catalogs, for the riz bands.

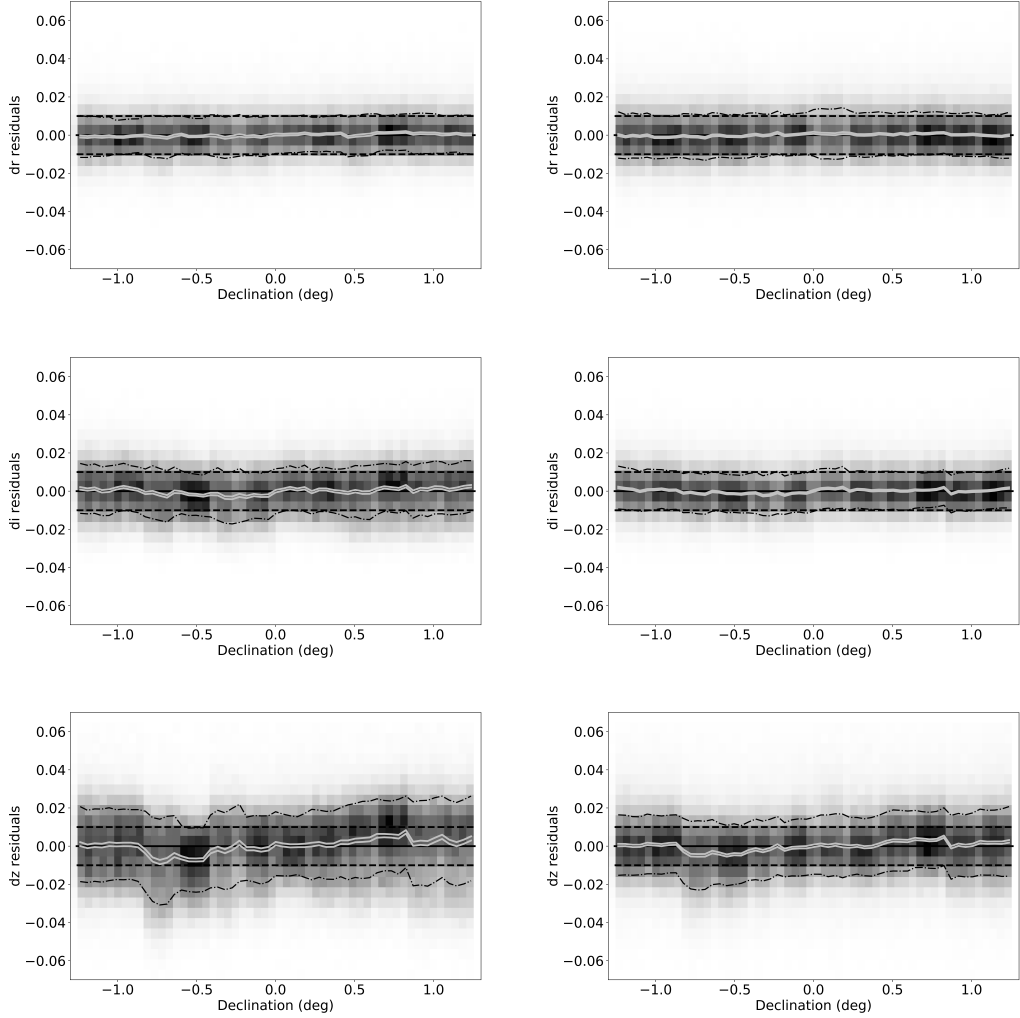


Figure 14. Analogous to Figure 13, except that magnitude differences are binned by Declination.

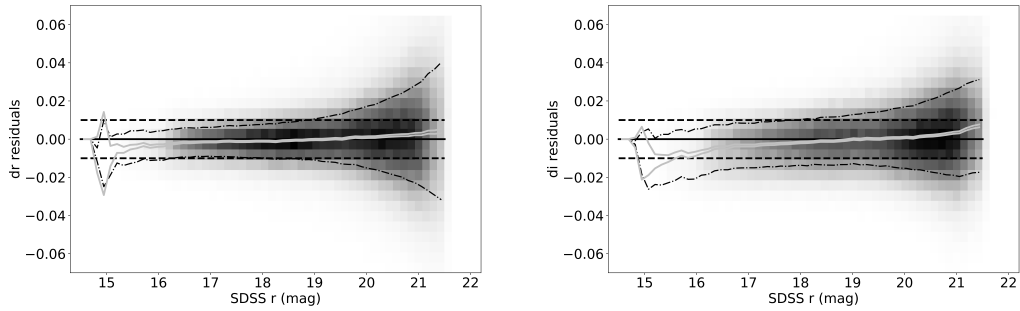


Figure 15. A comparison of the magnitude differences between the SDSS v3.4 catalog and DES catalog, for the *r* and *i* bands. Note the good agreement even at the faint end ($20 < r < 21$), where Gaia Gmag magnitudes appear too faint by about 0.02 mag (see Figure 4).

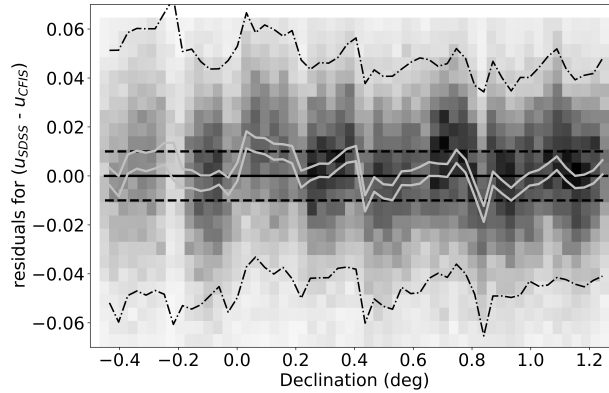


Figure 16. Analogous to Figure 6, except that here residuals between the SDSS u band magnitudes and u band magnitudes from the CFIS catalog (corrected for small color terms, ~ 0.05 mag, as a function of the $u - g$ color), for $\sim 150,000$ matched stars with $1.0 < u - g < 2.1$ and $r < 20$ are shown. The binned median scatter is 5.7 millimag. Note that the CFIS data are available only for Declination > -0.45 degree.

- Hunter, J. D. 2007, Computing In Science & Engineering, 9, 90, doi: [10.1109/MCSE.2007.55](https://doi.org/10.1109/MCSE.2007.55)
- Ivezić, Ž., Lupton, R. H., Schlegel, D., et al. 2004, Astronomische Nachrichten, 325, 583, doi: [10.1002/asna.200410285](https://doi.org/10.1002/asna.200410285)
- Ivezić, Ž., Smith, J. A., Miknaitis, G., et al. 2007, AJ, 134, 973
- Ivezić, Ž., Kahn, S. M., Tyson, J. A., et al. 2019, ApJ, 873, 111, doi: [10.3847/1538-4357/ab042c](https://doi.org/10.3847/1538-4357/ab042c)
- Jones, E., Oliphant, T., Peterson, P., et al. 2001–, SciPy: Open source scientific tools for Python.
<http://www.scipy.org/>
- Kaiser, N., Burgett, W., Chambers, K., et al. 2010, in Society of Photo-Optical Instrumentation Engineers (SPIE) Conference Series, Vol. 7733, Ground-based and Airborne Telescopes III, 77330E, doi: [10.1117/12.859188](https://doi.org/10.1117/12.859188)
- Oliphant, T. E. 2006, A guide to NumPy, Vol. 1 (Trelgol Publishing USA)
- Pier, J. R., Munn, J. A., Hindsley, R. B., et al. 2003, AJ, 125, 1559, doi: [10.1086/346138](https://doi.org/10.1086/346138)
- Smith, J. A., Tucker, D. L., Kent, S., et al. 2002, AJ, 123, 2121, doi: [10.1086/339311](https://doi.org/10.1086/339311)
- VanderPlas, J., Connolly, A. J., Ivezić, Ž., & Gray, A. 2012, in Proceedings of Conference on Intelligent Data Understanding (CIDU), pp. 47–54, 2012., 47–54, doi: [10.1109/CIDU.2012.6382200](https://doi.org/10.1109/CIDU.2012.6382200)
- York, D. G., Adelman, J., Anderson, John E., J., et al. 2000, AJ, 120, 1579, doi: [10.1086/301513](https://doi.org/10.1086/301513)

APPENDIX

A. APPENDIX INFORMATION

Here is Appendix A.